J|A|C|S
ARTICLES
Published on Web 04/19/2007

Design of a Hybrid Biosensor for Enhanced Phosphopeptide Recognition Based on a Phosphoprotein Binding Domain Coupled with a Fluorescent Chemosensor

Takahiro Anai, Eiji Nakata, Yoichiro Koshi, Akio Ojida, and Itaru Hamachi*

Contribution from the Department of Synthetic Chemistry and Biological Chemistry, Graduate School of Engineering, Kyoto University, Katsura Campus, Nishikyo-ku, Kyoto 615-8510, Japan

Received December 28, 2006; E-mail: ihamachi@sbchem.kyoto-u.ac.jp

Abstract: Protein-based fluorescent biosensors with sufficient sensing specificity are useful analytical tools for detection of biologically important substances in complicated biological systems. Here, we present the design of a hybrid biosensor, specific for a bis-phosphorylated peptide, based on a natural phosphoprotein binding domain coupled with an artificial fluorescent chemosensor. The hybrid biosensor consists of a phosphoprotein binding domain, the WW domain, into which has been introduced a fluorescent stilbazole having Zn(II)−dipicolylamine (Dpa) as a phosphate binding motif. It showed strong binding affinity and high sensing selectivity toward a specific bis-phosphorylated peptide in the presence of various phosphate species such as the monophosphorylated peptide, ATP, and others. Detailed fluorescence titration experiments clearly indicate that the binding-induced fluorescence enhancement and the sensing selectivity were achieved by the cooperative action of both binding sites of the hybrid biosensor, i.e., the WW domain and the Zn(II)−Dpa chemosensor unit. Thus, it is clear that the tethered Zn(II)−Dpa-stilbazole unit operated not only as a fluorescence signal transducer, but also as a sub-binding site in the hybrid biosensor. Taking advantage of its selective sensing property, the hybrid biosensor was successfully applied to real-time and label-free fluorescence monitoring of a protein kinase-catalyzed phosphorylation.

Introduction

Fluorescent sensors that can selectively detect a biologically important substance are powerful analytical tools for studying biological events.[1,2] Among a variety of such sensors, biosensors based on sophisticated protein functions have been widely applied to in vitro assays as well as bio-imaging studies in living cells.[3]

Biosensors are usually designed by combining a native protein domain with a fluorophore as a sensing unit, to transduce a substrate-binding event into a fluorescence signal. A representative class of biosensors employs a FRET (fluorescence resonance energy transfer) probe created by genetic fusion of a pair of fluorescent proteins such as CFP and YFP.[4] Another important class of biosensors is made by covalent modification of a protein with a small synthetic dye such as an environment-sensitive fluorophore.[5,6] In this class of biosensor, the fluorophore is usually tethered at the periphery of the active site of the protein so that it responds to substrate binding by changing its fluorescence intensity or wavelength. A variety of biosensors in these two categories have been developed, and their use in sensing various biological substrates and events has been demonstrated.

An alternative approach to the design of a fluorescent biosensor is the hybridization of a protein with an artificial chemosensor, which possesses a binding and sensing ability for

(1) (a) Geddes, C. D., Lakowicz, J. R., Eds. *Topics in Fluorescence Spectroscopy*; Kluwer Academic: New York, 2005; Vol. 9. (b) Geddes, C. D., Lakowicz, J. R., Eds. *Topics in Fluorescence Spectroscopy*; Kluwer Academic: New York, 2005; Vol. 10. (c) Martínez-Máñez, R.; Sancenón, F. *Chem. Rev.* **2003**, *103*, 4419. (d) Callan, J. F.; de Silva, A. P.; Magri, D. C. *Tetrahedron* **2005**, *61*, 8551. (e) Giepmans, B. N. G.; Adams, S. R.; Ellisman, M. H.; Tsien, R. Y. *Science* **2006**, *312*, 217.

(2) (a) Peczuh, M. W.; Hamilton, A. D. *Chem. Rev.* **2000**, *100*, 2479. (b) Lavigne, J. J.; Anslyn, E. V. *Angew. Chem., Int. Ed.* **2001**, *40*, 3118. (c) Beer, P. D.; Gale, P. A. *Angew. Chem., Int. Ed.* **2001**, *40*, 486. (d) Kruppa, M.; Konig, B. *Chem. Rev.* **2006**, *106*, 3520. (e) Mancin, F.; Rampazzo, E.; Tecilla, P.; Tonellato U. *Chem. Eur. J.* **2006**, *12*, 1844. (f) Mohr, G. J. *Anal. Bioanal. Chem.* **2006**, *386*, 1201. (g) O'Neil, E. J.; Smith, B. D. *Coord. Chem. Rev.* **2006**, *250*, 3068.

(3) (a) Dwyer, M. A.; Hellinga, H. W. *Curr. Opin. Struct. Biol.* **2004**, *14*, 295. (b) Jelinek, R.; Kolusheva, S. *Chem. Rev.* **2004**, *104*, 5987. (c) Willner, I.; Katz, E. *Angew. Chem., Int. Ed.* **2000**, *39*, 1180. (d) Shaner, N. C., Steinbach, P. A.; Tsien, R. Y. *Nat. Methods* **2005**, *2*, 905. (e) Umezawa, Y. *Chem. Asian J.* **2006**, *1*, 304.

(4) (a) Miyawaki, A.; Llopis, J.; Helm, R.; McCaffery, M. J.; Adams, J. A.; Ikura, M.; Tsien, R. Y. *Nature* **1997**, *388*, 882. (b) Romoser, V. A.; Hinkle, P. M.; Persechini, A. *J. Biol. Chem.* **1997**, *272*, 13270. (c) Truong, K.; Sawano, A.; Mizuno, H.; Hama, H.; Tong, K. I.; Mal, T. K.; Miyawaki, A.; Ikura, M. *Nat. Struct. Biol.* **2001**, *8*, 1069. (d) Gaits, F. G.; Hahn, K. *Sci., STKE* **2003**, pe3. (e) Kiyokawa, E.; Hara, S.; Nakamura, T.; Matsuda, M. *Cancer Sci.* **2006**, *97*, 8−15.

(5) (a) Morii, T.; Sugimoto, K.; Makino, K.; Otsuka, M.; Imoto, K.; Mori, Y. *J. Am. Chem. Soc.* **2002**, *124*, 1138. (b) Sugimoto, K.; Nishida, M.; Otsuka, M.; Makino, K.; Ohkubo, K.; Mori, Y.; Morii, T. *Chem. Biol.* **2004**, *11*, 475. (c) Toutchkine, A.; Kraynov, V.; Hahn, K. *J. Am. Chem. Soc.* **2003**, *125*, 4132. (d) Chan, P. H.; Liu, H. B.; Chen, Y. W.; Chan, K. C.; Tsang, C. W.; Leung, Y. C.; Wong, K. Y. *J. Am. Chem. Soc.* **2004**, *126*, 4074. (e) Nalbant, P.; Hodgson, L.; Kraynov, V.; Toutchkine, A.; Hahn, K. M. *Science* **2004**, *305*, 1615. (f) Vazquez, M. E.; Blanco, J. B.; Imperiali, B. *J. Am. Chem. Soc.* **2005**, *127*, 1300. (9) Cohen, B. E.; Pralle, A.; Yao, X.; Swaminath, G.; Gandhi, C. S.; Jan, Y. N.; Kobilka, B. K.; Isacoff, E. Y.; Jan, L. Y. *Proc. Natl. Acad. Sci. U.S.A.* **2005**, *102*, 965.

(6) (a) Hamachi, I.; Nagase, T.; Shinkai, S. *J. Am. Chem. Soc.* **2000**, *122*, 12065. (b) Nagase, T.; Shinkai, S.; Hamachi, I. *Chem. Commun.* **2001**, *3*, 229. (c) Nagase, T.; Nakata, E.; Shinkai, S.; Hamachi, I. *Chem. Eur. J.* **2003**, *9*, 3660. (d) Koshi, Y.; Nakata, E.; Hamachi, I. *ChemBioChem* **2005**, *6*, 1349. (e) Nakata, E.; Koshi, Y.; Koga, E.; Katayama, Y.; Hamachi, I. *J. Am. Chem. Soc.* **2005**, *127*, 13253. (g) Takaoka, Y.; Tsutsumi, H.; Kasagi, N.; Nakata, E.; Hamachi, I. *J. Am. Chem. Soc.* **2006**, *128*, 3273.

10.1021/ja0693284 CCC: $37.00 **© 2007 American Chemical Society**

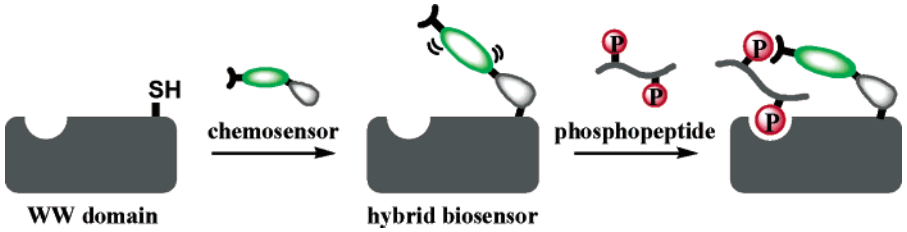

Figure 1. Construction of the hybrid biosensor and fluorescence sensing for the doubly phosphorylated peptide discussed in this study.

the protein substrate.[7] By the cooperative action of both protein and chemosensor unit, the hybrid biosensor can potentially provide a binding affinity higher than that of the native protein, for a specific substrate. Such a facilitated function could not be expected in the conventional biosensors mentioned above. In addition, the hybrid approach might dramatically modulate the substrate binding selectivity so as to provide a biosensor capable of binding to a certain biological substrate that could not be recognized beforehand by the native protein.[8,9] In these ways, this approach might greatly expand the scope of fluorescence analysis using biosensors. Irrespective of this potential, there has not yet been much exploration of hybrid biosensors.

Post-translational modification of proteins by phosphorylation is a ubiquitous regulatory mechanism of diverse protein functions and plays a central role in the control of cellular signaling networks.[10] Protein phosphorylation regulates mainly the enzymatic activity of proteins,[11] and also the reversible assembly of proteins into signaling complexes, by interactions at the phosphoprotein binding domain.[12] To elucidate such important roles of protein phosphorylation, it is desirable to develop fluorescence sensing systems for phosphoproteins involved in signal transduction. To date, a number of biosensors for protein kinase activity have been developed, including fluorescent protein (GFPs)-based FRET probes[13] or biosensors having a synthetic fluorophore.[14] In these biosensors, a sensing module is covalently attached to a reactive module within one protein molecule. Thus, these can sense only their own phosphorylation/dephosphorylation but not that of a natural, underivatized phosphorylated peptide or protein. On the other hand, methods for directly sensing a phosphoprotein using artificial sensors are still poorly developed. We have recently reported the first artificial chemosensors for a phosphorylated protein surface using coordination chemistry.[15] Although these chemosensors could bind selectively to a phosphate anion derivative in aqueous medium and showed a distinctive fluorescence increase upon binding to phosphorylated peptides or proteins, their selectivity among many phosphorylated substances was not sufficient.

In this report, we describe the design of a fluorescent hybrid biosensor for a specific phosphorylated peptide. Introduction of an artificial chemosensor into a phosphoprotein binding domain provides the hybrid biosensor with a strong binding affinity and high sensing selectivity toward the specific bisphosphorylated peptide even in the presence of various phosphate anion species (Figure 1). Taking advantage of the selective sensing function, the hybrid biosensor was successfully applied to real-time and label-free fluorescence monitoring of kinase-catalyzed phosphorylation.

Molecular Design of the Biosensor Hybridized with the Artificial Chemosensor

The group IV WW domain is a small binding motif capable of selectively binding to phosphorylated proline-rich sequences, especially to a pSer-Pro or pThr-Pro.[16] In this study, the WW domain (6−39 residues) derived from Pin1 protein[17] was used as a binding scaffold of the hybrid biosensor (Figure 2a). It was reported that the Pin1 protein selectively binds to the multiphosphorylated C-terminal domain (CTD) repeat sequence of RNA polymerase II through the WW domain and regulates the transcriptional activity of living cells. X-ray crystallographic analysis of the Pin1 WW domain complexed with a doubly

(7) (a) Gu, L.-Q.; Braha, O.; Conlan, S.; Cheley, S.; Bayley, H. *Nature* **1999**, *398*, 686. (b) Bayley, H.; Cremer, P. S. *Nature* **2001**, *413*, 226.
(8) (a) Muranaka, N.; Hohsaka, T.; Sisido, M. *FEBS Lett.* **2002**, *510*, 10. (b) Banghart, M.; Borges, K.; Isacoff, E.; Trauner, D.; Kramer, R. H. *Nat. Neurosci.* **2004**, *7*, 1381. (c) Endo, M.; Nakayama, K.; Kaida, Y.; Majima, T. *Angew. Chem., Int. Ed.* **2004**, *43*, 5643−5645. (d) Koçer, A.; Walko, M.; Meijberg, W.; Feringa, B. L. *Science* **2005**, *309*, 755. (e) Volgraf, M.; Gorostiza, P.; Numano, R.; Kramer, R. H.; Isacoff, E. Y.; Trauner, D. *Nat. Chem. Biol.* **2006**, 2, 47. (f) Muramatsu, S.; Kinbara, K.; Taguchi, H.; Ishii, N.; Aida T. *J. Am. Chem. Soc.* **2006**, *128*, 3764.
(9) Nakata, E.; Nagase, T.; Shinkai, S.; Hamachi, I. *J. Am. Chem. Soc.* **2004**, *126*, 490.
(10) (a) Pawson, T.; Scott, J. D. *Trends Biochem. Sci.* **2005**, *30*, 286. (b) Johnson, S. A.; Hunter, T. *Nat. Methods* **2005**, *2*, 17. (c) Sefton, B. M.; Hunter, T. *Protein Phosphorylation*; Academic Press: New York, 1998.
(11) Johnson, L. N.; Lewis, R. J. *Chem. Rev.* **2001**, *101*, 2209.
(12) (a) Yaffe, M. B. *Nat. Rev. Mol. Cell Biol.* **2002**, *3*, 177. (b) Yaffe, M. B.; Elia, A. *Curr. Opin. Cell Biol.* **2001**, *13*, 131. (c) Pawson, T.; Gish, G. D.; Nash, P. *Trends Cell Biol.* **2001**, *11*, 504. (d) Pawson, T.; Raina, M.; Nash, P. *FEBS Lett.* **2002**, *513*, 2.
(13) (a) Nagai, Y.; Miyazaki, M.; Aoki, R.; Zama, T.; Inouye, S.; Hirose, K.; Iino, M.; Hagiwara, M. *Nat. Biotechnol.* **2000**, *18*, 313. (b) Kurokawa, K.; Mochizuki, N.; Ohba, Y.; Mizuno, H.; Miyawaki, A.; Matsuda, M. *J. Biol. Chem.* **2001**, *276*, 31305. (c) Ting, A. Y.; Kain, K. H.; Klemke, R. L.; Tsien, R. Y. *Proc. Natl. Acad. Sci. U.S.A.* **2001**, *98*, 15003. (d) Zhang, J.; Ma, Y.; Taylor, S. S.; Tsien, R. Y. *Proc. Natl. Acad. Sci. U.S.A.* **2001**, *98*, 14997. (e) Sato, M.; Ozawa, T.; Inukai, K.; Asano, T.; Umezawa, Y. *Nat. Biotechnol.* **2002**, *20*, 287.
(14) (a) Shults, M. D.; Imperiali, B. *J. Am. Chem. Soc.* **2003**, *125*, 14248. (b) Lawrence, D. S. *Acc. Chem. Res.* **2003**, *36*, 401. (c) Turk, B. E. *Nat. Method* **2005**, *2*, 251. (d) Rothman, D. M.; Shults, M. D.; Imperiali, B. *Trends Cell Biol.* **2005**, *15*, 502. (e) Schults, M. D.; Janes, K. A.; Lauffenburger, D. A.; Imperiali, B. *Nat. Methods* **2005**, *2*, 277. (f) Sun, H.; Low, K. E.; Woo, L. S.; Noble, R. L.; Graham, R. J.; Connaughton, S. S.; Gee, M. A.; Lee, L. G. *Anal. Chem.* **2005**, *77*, 2043. (g) Balakrishnan, S.; Zondlo, N. J. *J. Am. Chem. Soc.* **2006**, *126*, 5590. (h) Wang, Q.; Cahill, S. M.; Blumenstein, M.; Lawrence, D. S. *J. Am. Chem. Soc.* **2006**, *128*, 1808. (i) Sculimbrene, B. R.; Imperiali, B. *J. Am. Chem. Soc.* **2006**, *128*, 7346.
(15) (a) Ojida, A.; Hamachi, I. *Bull. Chem. Soc. Jpn.* **2006**, *79* 35. (b) Ojida, A.; Miyahara, Y.; Kohira, T.; Hamachi, I. *Biopolymers (Pept. Sci.)* **2004**, *76*, 177. (c) Ojida, A.; Inoue, M.; Mito-oka, Y.; Tsutsumi, H.; Sada, K.; Hamachi, I. *J. Am. Chem. Soc.* **2006**, *128*, 2052. (d) Ojida, A.; Mito-oka, Y.; Sada, K.; Hamachi, I. *J. Am. Chem. Soc.* **2004**, *126*, 2454. (e) Ojida, A.; Kohira, T.; Hamachi, I. *Chem. Lett.* **2004**, *33*, 1024. (f) Ojida, A.; Inoue, M.; Mito-oka, Y.; Hamachi, I., *J. Am. Chem. Soc.* **2003**, *125*, 10184. (g) Ojida, A.; Mito-oka, Y.; Inoue, M.; Hamachi, I. *J. Am. Chem. Soc.* **2002**, *124*, 6256.
(16) (a) Sudol, M.; Sliwa, K.; Russo, T. *FEBS Lett.* **2001**, *490*, 190. (b) Zarrinpar, A.; Lim, W. A. *Nat. Struct. Biol.* **2000**, *7*, 611. (c) Yan, K. S.; Kuti, M.; Zhou, M.-M. *FEBS Lett.* **2002**, *513*, 67. (d) Ball, L. J.; Kühne, R.; Schneider-Mergener, J.; Oschkinat, H. *Angew. Chem., Int. Ed.* **2005**, *44*, 2852.
(17) (a) Verdecia, M. A.; Bowman, M. E.; Lu, K. P.; Hunter, T.; Noel, J. P. *Nat. Struct. Biol.* **2000**, *7*, 639. (b) Xu, Y.-X.; Hirose, Y.; Zhou, X. Z.; Lu, K. P.; Manley, J. L. *Genes Dev.* **2003**, *17*, 2765. (c) Lu, P.-J.; Zhou, X.-Z.; Liou, Y.-C.; Noel, J.-P.; Lu, K.-P. *J. Biol. Chem.* **2002**, *277*, 2381. (d) Wintjens, R.; Wieruszeski, J.-M.; Drobecq, H.; Rousselot-Pailley, P.; Buée, L.; Lippens, G.; Landrieu, I. *J. Biol. Chem.* **2001**, *276*, 25150. (e) Jäger, M.; Nguyen, H.; Crane, J. C.; Kelly, J. W.; Gruebele, M. *J. Mol. Biol.* **2001**, *311*, 373.

a) native WW domain : KLPPGWEKRMSRSSGRVYYFNHITNASQWERPSG

6 10 20 30

E12C-WW : KLPPGWCKRMSRSSGRVYYFNHITNASQWERPSG

R14C-WW : KLPPGWEKCMSRSSGRVYYFNHITNASQWERPSG

M15C-WW : KLPPGWEKRCSRSSGRVYYFNHITNASQWERPSG

b)

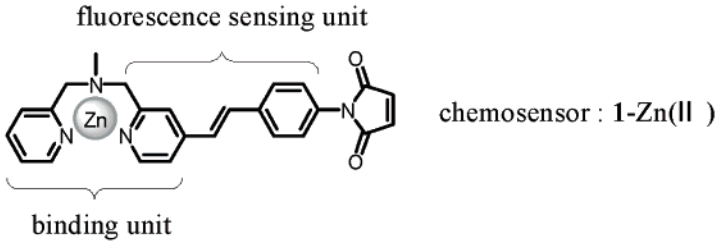

c)

pS2,5-CTD : H-YpSPTpSPS-NH_2

pS6,9-CTD : H-TSPSYpSPTpSPS-NH_2

pS6-CTD : H-TSPSYpSPTSPS-NH_2

pS9-CTD : H-TSPSYSPTpSPS-NH_2

S-CTD : H-TSPSYSPTSPS-NH_2

IRK1P : AcHN-TRDIpYETDYYRL-NH_2

IRK2P : AcHN-TRDIpYETDpYYRL-NH_2

Figure 2. (a) Amino acid sequences of the WW domain and its mutants. (b) Molecular structure of **1**−2Zn(II). (c) Amino acid sequences of the phosphorylated peptides.

Scheme 1. Synthesis of **1**(Zn)[a]

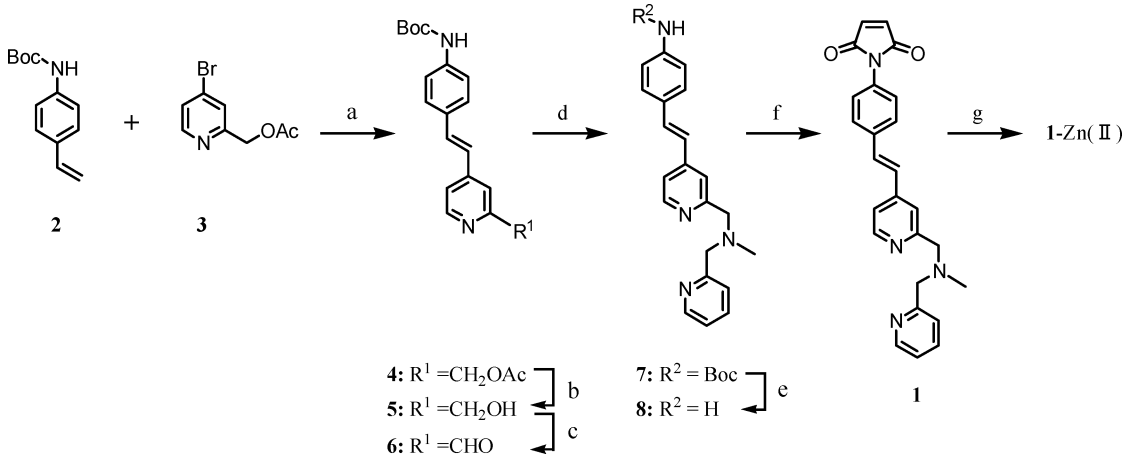

[a] Reagents and conditions: (a) $Pd(OAc)_2$, PPh_3, DMF, 80 °C. (b) 1 N NaOH, MeOH, rt. (c) MnO_2, THF, rt to 45 °C. (d) Methylpyridine-2-ylmethylamine·HCl, $NaBH(OAc)_3$, AcOH, CH_2Cl_2, rt. (e) TFA, CH_2Cl_2, rt. (f) Maleic anhydride, THF, 40 °C, and then Ac_2O, AcONa, 60 °C. (g) $Zn(NO_3)_2$, MeOH, rt.

phosphorylated pS2,5-CTD peptide (YpSPTpSPS, Figure 2c) revealed that the WW domain tightly interacts with one phosphorylated serine pS5, but not with another pS2.[17a] Thus, it was expected that introduction of an artificial chemosensor unit that is able to bind and fluorescently sense the pS2 residue would provide a hybrid biosensor that exerts an enhanced binding affinity and sensing selectivity for the multiphosphorylated CTD sequence.

We have recently demonstrated that the zinc complex of 2,2′-dipicolylamine (Zn(II)−Dpa) is an effective binding motif for phosphate anions.[15] On the basis of this finding, **1**−Zn(II) was designed as an artificial chemosensor to be coupled with the WW domain (Figure 2b). It is well-known that the fluorescence quantum yield of stilbazole derivatives is largely affected by the torsional rotational freedom of the two aromatic groups.[18] Thus, it is reasonable that the cooperative interaction of both phosphate groups of the pS-6,9 sequence with the hybrid biosensor might induce the fluorescence intensity change of **1**−Zn(II) due to the conformational restriction of the stilbazole moiety. The maleimide group was attached to the stilbazole unit of **1**−Zn(II) as a reactive site for the cysteine residue that is mutationally introduced to the WW domain. The chemosensor **1**−Zn(II) was synthesized by the synthetic route in Scheme 1 and characterized by ^{1}H NMR, elemental analysis, and FAB-MS.

(18) (a) Pyun, C. H.; Lyle, T. A.; Daub, G. H.; Park, S. M. *Chem. Phys. Lett.* **1986**, *124*, 48. (b) Rosania, G. R.; Lee, J. W.; Ding, L.; Yoon, H. S.; Chang, Y. T. *J. Am. Chem. Soc.* **2003**, *125*, 1130.

Preparation of Hybrid Biosensor. The crystallographic structure of the complex of Pin1 WW domain with the phosphorylated CTD peptide (pS2,5-CTD, Figure 2c) shows that the side chains of Glu12, Arg14, and Met15 of the WW domain are rather close to the phosphate group of pS2 of the CTD peptide.[17a] This structural information implied that these positions are suitable candidates for incorporation of the artificial chemosensor **1**−Zn(II) as a binding unit for pS2. Thus, three WW domain mutants (E12C-WW, R14C-WW, and M15C-WW, Figure 2a) possessing a cysteine at the 12, 14, or 15 position, respectively, were prepared by solid-phase peptide synthesis, purified by HPLC, and characterized by MALDI-TOF-mass spectroscopy (MALDI-TOF-MS). Introduction of **1**−Zn(II) into E12C-WW and M15C-WW was carried out by simple incubation of the corresponding Cys-mutant and **1**−Zn(II) in HEPES buffer solution. The coupling reaction was complete within 2 h under mild conditions (pH 7.2, 25 °C) in both cases. This was confirmed by MALDI-TOF-MS that traced the adduct formation as well as the concomitant disappearance of the mutant WW domain (Figure S1). After purification with size-exclusion gel chromatography, the hybrid biosensors (**1**(Zn)−E12C-WW and **1**(Zn)−M15C-WW) were tested for the fluorescence sensing. Conjugation of R14C-WW with **1**−Zn(II) was not done because this mutant did not form a native-like folded structure (vide infra).

The structure of these hybrid biosensors was investigated by circular dichroism (CD) spectroscopy prior to evaluation of their fluorescence-sensing capabilities (Figure 3). It is known that native WW domains show a characteristic positive Cotton peak at 227 nm due to the folded structure.[19] Among the three Cys-mutants, E12C-WW and M15C-WW showed the characteristic CD peak at 227 nm identical with native WW. However, in the case of the mutant R14C-WW, this peak was completely absent, indicating that this mutant does not retain a native-like structure. This can be explained by the side chain of Arg14 playing an important role in the formation of the secondary structure of the WW domain by participating in both the hydrophobic cluster and the hydrogen-bonding network with other amino acid residues.[17e] The structure of the hybrid biosensors were also investigated by CD measurements. **1**(Zn)−M15C-WW showed a CD spectrum almost identical with that of the native WW domain (Figure 3b), indicating that attachment of the artificial chemosensor unit did not disturb the native-like folded structure in this hybrid biosensor. In contrast, in the case of **1**(Zn)−E12C-WW, the CD signal in this region completely disappeared, suggesting that the introduction of **1**−Zn(II) on the surface of the mutant E12C-WW significantly affects the folded structure destroying the native-like conformation. Thus, the subsequent experiments were carried out using **1**(Zn)−M15C-WW as the hybrid biosensor.

Fluorescence Sensing of Phosphorylated Derivatives. On excitation at 340 nm, **1**(Zn)−M15C-WW showed fluorescence emission with a maximum at 440 nm (Figure S2). This emission is ascribed to the stilbazole fluorophore of the artificial chemosensor incorporated into **1**(Zn)−M15C-WW. When the bis-phosphorylated pS6,9-CTD peptide, an analogue of pS2,5-CTD peptide, was added to a solution of **1**(Zn)−M15C-WW, the fluorescence intensity at 440 nm increased as shown in Figure 4a (F_{max}/F_{int} = 1.6, Figure 4a). This suggested the binding-induced conformational rigidification of the stilbazole fluorophore, according to the design principle. Fluorescence Job's plot showed that their binding stoichiometry is 1:1 (inset of Figure 4a). The increase at 440 nm showed typical saturation behavior (Figure 4b) with a binding constant of 1.2×10^6 M^{-1} analyzed by the nonlinear curve-fitting method. This value is ~10-fold larger than that of native WW domain ($K_{app} = 1.4 \times 10^5$ M^{-1})[15c,20] and ~1000-fold larger than that of the mononuclear zinc complex of **1**−Zn(II).[21] These results suggest that both binding sites of **1**(Zn)−M15C-WW, i.e., those for the zinc complex and the WW domain, cooperatively interact with the two phosphate groups of pS6,9-CTD peptide so as to yield the stronger binding compared to binding through the individual interaction.

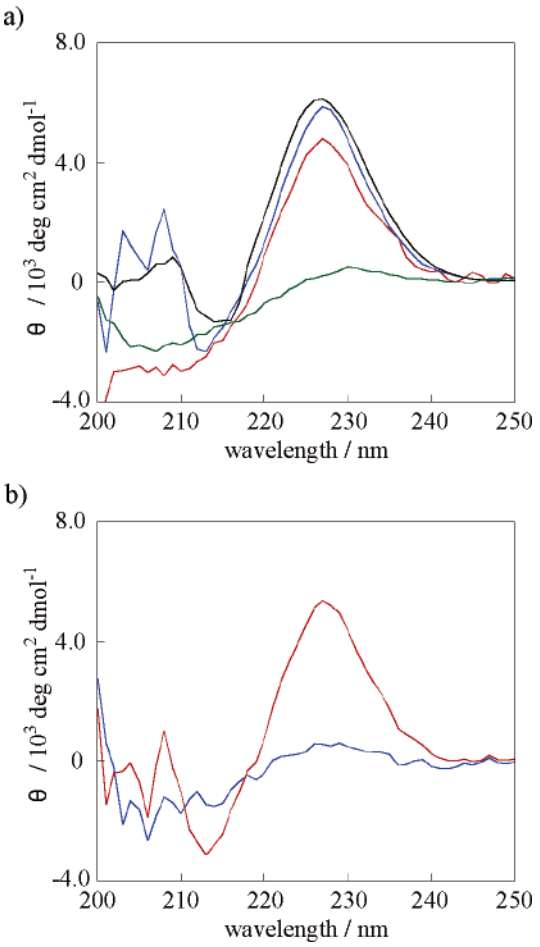

Figure 3. (a) Circular dichroism (CD) spectra of the mutant WW domains; native WW (black line), E12C-WW (blue line), R14C-WW (green line), and M15C-WW (red line). (b) Circular dichroism (CD) spectra of the WW domains hybridized with **1**−Zn(II), **1**(Zn)−M15C-WW (red line), **1**(Zn)−E12C-WW (blue line), 20 mM potassium phosphate buffer solution (pH 7.2), 20 mM NaCl, 4 °C.

The fluorescence sensing ability of **1**(Zn)−M15C-WW was further explored for other phosphate derivatives (Figure 5 and Figure S3). It is noteworthy, in particular, that the binding constant for IRK2P, a bis-phosphorylated fragment of insulin-recep-

(19) (a) Kaul, R.; Angeles, A. R.; Jager, M.; Powers, E. T.; Kelly, J. W. *J. Am. Chem. Soc.* **2001**, *123*, 5206. (b) Kaul, R.; Deechongkit, S.; Kelly, J. W. *J. Am. Chem. Soc.* **2002**, *124*, 11900.

(20) The binding affinity of the native WW domain was determined by the fluorescence polarization assay with the rhodamine-labeled pS6,9-CTD peptide, experimental details of which are described in reference 15c.

(21) The binding affinity of **1**−Zn(II) with the bis-phosphorylated pS6,9-CTD or mono-phosphorylated pS6-CTD peptide was determined by ITC (isothermal titration calorimetry) experiment (see Figure S5).

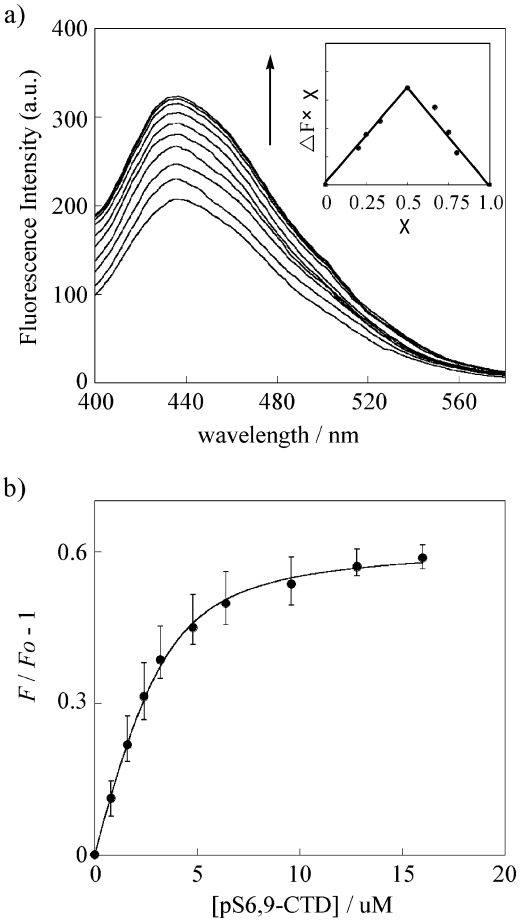

Figure 4. (a) Fluorescence spectral change of **1**(Zn)−M15C-WW upon addition of the doubly phosphorylated pS6,9-CTD peptide (0−16 μM). [**1**(Zn)−M15C-WW] = 3.2 μM, 50 mM HEPES buffer solution (pH 7.2), 15 ± 1 °C, λ_{ex} = 340 nm. (Inset) Job plot fluorescently examined between **1**(Zn)−M15C-WW and pS6,9-CTD peptide (total concentration is 10 μM). (b) Fluorescence titration curve of **1**(Zn)−M15C-WW with pS6,9-CTD peptide measured in (a). All data points are mean ± sem obtained by the individual three experiments.

tor kinase (1156−1164, Figure 2),[22] is in the range of 10^4 (M^{-1}). This affinity is much smaller than that for pS6,9-CTD peptide, and is almost the same as that for monophosphorylated IRK1P or pS6-CTD peptide. This is because the IRK peptide does not show affinity for the WW domain, which gives rise to the high sequence selectivity of the present **1**(Zn)−M15C-WW. Similarly, the binding affinity of **1**(Zn)−M15C-WW for nucleoside pyrophosphates such as ATP or ADP is significantly lower than that of pS6,9-CTD peptide (Table 1). Thus, it is concluded that **1**(Zn)−M15C-WW is a fluorescent biosensor selective for bisphosphorylated pS6,9-CTD peptide among various other phosphate derivatives.

The fluorescence polarization assay additionally gave us the sensing mechanism of **1**(Zn)−M15C-WW for the phosphorylated derivatives. Upon complexation with pS6,9-CTD peptide, the fluorescence anisotropy value (*r*) of **1**(Zn)−M15C-WW gradually increased from 0.3 to 0.36 (Figure S4). Curve-fitting analysis of this change gave a binding constant of 5.8×10^5 M^{-1}, almost identical with that from the fluorescence titration (Table 1, Figure 5). The increase in *r* value implies suppressed mobility of the fluorophore, and thus it supports a proposed

Table 1. Summary of the Binding Constants of **1**(Zn)−M15C-WW or Native WW Domain for Various Phosphorylated Derivatives

	K_{app}/M^{-1}		
substrate	**1**(Zn)–M15C-WW[a]		native WW domain[b]
pS6,9-CTD	1.2×10^6	(5.8×10^5)	1.4×10^5
pS6-CTD	3.4×10^4	(9.9×10^4)	6.8×10^4
pS9-CTD	*c*		1.3×10^5
S-CTD	*c*		*c*
IRK1P	5.6×10^4		
IRK2P	7.6×10^4		
ATP	6.0×10^4		
ADP	4.9×10^4		
PhP	4.3×10^4	(6.3×10^4)	

[a] Determined by the fluorescence titration. The binding constants in parentheses were obtained by the fluorescence polarization assay. [b] Determined by the fluorescence polarization assay with the rhodamine-labeled phosphopeptide. [c] Not determined due to small fluorescence intensity or anisotropy value change.

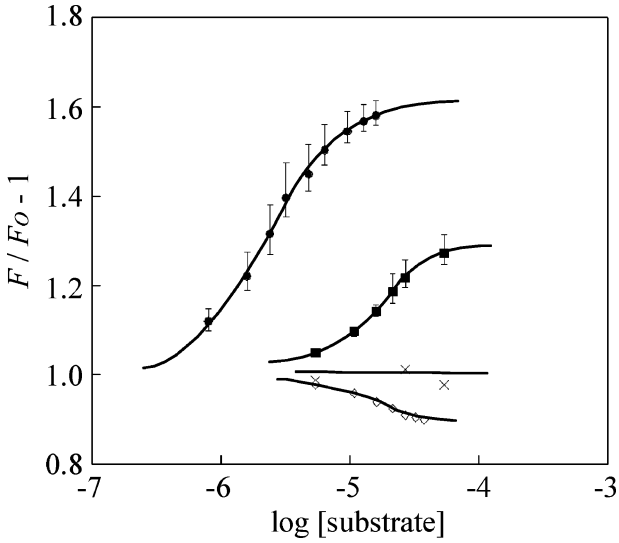

Figure 5. Fluorescence titration profiles of **1**(Zn)−M15C-WW at the emission of 440 nm with the various CTD peptides; pS6,9-CTD (●), pS6-CTD (■), pS9-CTD (◇), and S-CTD peptide (×) in 50 mM HEPES buffer solution (pH 7.2), 15 ± 1 °C, λ_{ex} = 340 nm.

sensing mechanism, in which the conformational rigidification of the stilbazole moiety induces the fluorescence enhancement upon two-point binding of **1**(Zn)−M15C-WW to pS6,9-CTD. The chemosensor **1**−Zn(II) itself, which is not conjugated with the WW domain, did not show any fluorescence change upon addition of excess pS6,9-CTD peptide or ATP (data not shown), also suggesting that the conformational restriction by bridging two pS units of CTD peptide through the Zn(Dpa) site and WW domain is an important factor in the selective fluorescence sensing by **1**(Zn)−M15C-WW.[23]

Figure 6 shows a computationally predicted structure of the binding complex between **1**(Zn)−M15C-WW and pS6,9-CTD peptide on the basis of the crystallographic structure of the native WW domain complexed with pS2,5-CTD peptide.[17a,24] In the

(22) Hubbard, S. R. *EMBO J.* **1997**, *16*, 5572.

(23) The moderate increases of fluorescence intensity (Figure 5) and *r* value (Figure S4) upon binding to pS6-CTD peptide suggest that **1**(Zn)−M15C-WW recognizes pS6-CTD peptide in a cooperative binding mode, in which the pS6 phosphate group and the non-phosphorylated proline-rich sequence (PTSP) are recognized by the Zn(II)−Dpa site and the WW domain of **1**(Zn)−M15C-WW, respectively. This is supported by the fact that the native WW domain binds to pS2-CTD peptide (YpSPTSPS) with a moderate binding afffinity ($K_{app} = 9 \times 10^3$ M^{-1}, see reference 17a).

(24) Structure of **1**−(Zn)−M15C-WW was minimized using Macro Model 8.5 (MMFFs force field). Calculation was applied with Molecular Mechanics (MM) and Molecular Dynamics (MD).

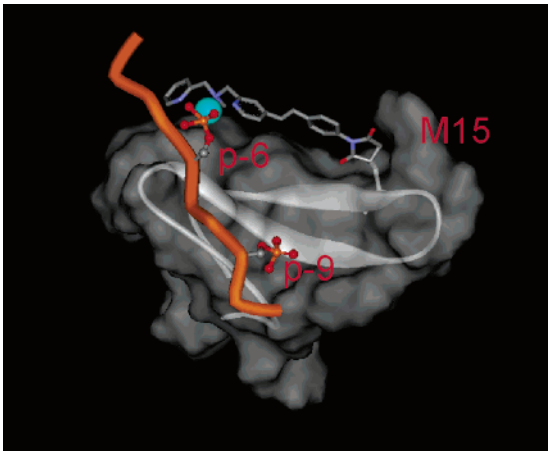

Figure 6. Computationally predicted structure of the binding complex between **1**(Zn)−M15C-WW (white ribbon with gray surface) and pS6,9-CTD peptide (orange solid bar).

calculated structure, the stilbazole moiety reaches from the Cys15 residue along the β-sheet of the WW domain, and it can be seen that the Zn(II)−Dpa site can bind to the phosphate group of pS-6 without interfering with other intrinsic interactions between pS-9 and the WW domain. Therefore, it is reasonable that such cooperative two-point binding with the two phosphate residues largely contributes to the selective sensing of the pS6,9-CTD peptide as well as the fluorescence enhancement.

Fluorescence Monitoring of Kinase-Catalyzed Phosphorylation. As mentioned above, the hybrid biosensor 1(Zn)−M15C-WW can selectively detect the bis-phosphorylated peptide sequence (pS6,9-CTD) even in the presence of other phosphorylated derivatives. Taking advantage of this selective sensing, we subsequently applied the hybrid biosensor for a fluorescence real-time assay of kinase-catalyzed peptide phosphorylation. Cyclin-dependent protein kinase 9 (CDK9) is an enzyme which phosphorylates the serine residues of the CTD sequence of RNA polymerase II as an active complex with cyclin T1 and plays an important role in controlling the cell transcriptional activity.[25]

In the phosphorylation assay, pS9-CTD peptide was employed as a substrate, and the phosphorylation event at Ser6 was fluorescently monitored using 1(Zn)−M15C-WW. Upon addition of CDK9/T1 kinase to a solution of pS9-CTD peptide and ATP, the fluorescence intensity of **1**(Zn)−M15C-WW gradually increased in a time-dependent manner as shown in Figure 7. To confirm the reaction progress, we separately checked the formation of pS6,9-CTD peptide by MALDI-TOF-MS by sampling the solution (data not shown). The initial rate of the fluorescence change apparently depends on the concentration of the substrate, pS9-CTD peptide. In control experiments, the fluorescence intensification was not observed in the absence of ATP, pS-9 CTD peptide, or CDK9/T1kinase. These results clearly indicate that **1**(Zn)−M15C-WW can successfully monitor the CDK9/T1 kinase-catalyzed phosphorylation reaction in real-time and in the absence of label, by selective detection of pS6,9-CTD peptide in the presence of other phosphorylated species such as the substrate pS9-CTD peptide, ATP, and ADP. The emission change data obtained with different substrate concentrations were analyzed by a Lineweaver−Burk plot to give, $K_m = (5.1 \pm 2.8) \times 10^{-4}$ M and $V_{max} = (4.0 \pm 1.4) \times 10^{-5}$ M·min^{-1}. The fluorescence assay was also conducted using non-phosphorylated CTD peptide (S-CTD peptide, Figure 2c) as a substrate under the same conditions, where phosphorylation occurred at the Ser-6 residue to produce pS6-CTD peptide.[26] However, it is interesting that no fluorescence change took place in this case (data not shown). This is attributed to the binding affinity with pS6-CTD peptide ($K_{app} = 3.4 \times 10^4$ M^{-1}) being too weak to monitor by fluoresence the kinase-catalyzed phosphorylation, demonstrating the substrate-selective sensing feature of the hybrid biosensor in the kinase reaction.

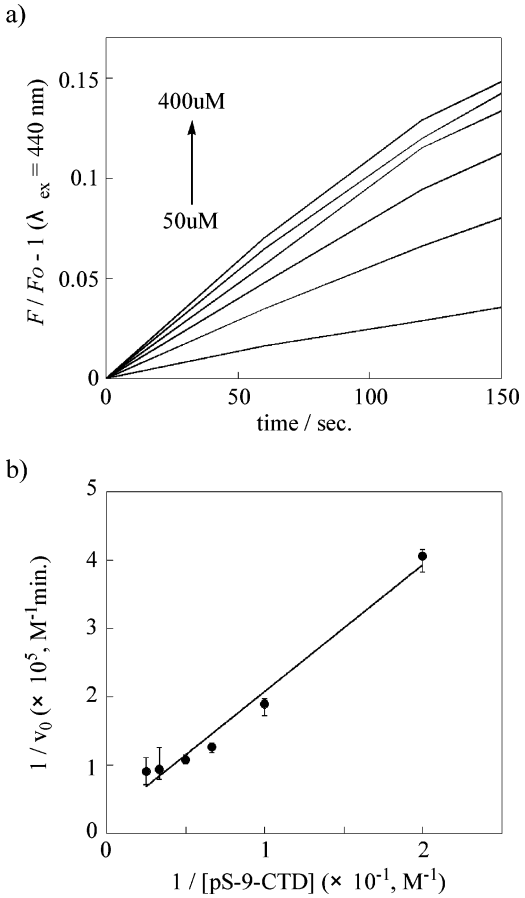

Figure 7. (a) Real-time fluorescence monitoring of CDK9/T1-catalyzed phosphorylation of pS9-CTD peptide (50, 100, 150, 200, 300, 400 μM) with **1**(Zn)−M15C-WW. (b) Lineweaver−Burk plot of the phosphorylation of pS9-CTD peptide catalyzed by CDK9/T1.

Conclusion

In summary, we have extended the validity of the hybrid approach for design of the fluorescence biosensor for phosphopeptides. The hybrid biosensor based on the WW domain and Zn(II)−Dpa chemosensor showed a strong binding affinity and high sensing selectivity for the specific bis-phosphorylated peptide, which distinguishes it from monophosphorylated peptides and other phosphorylated species. This enabled the hybrid biosensor to be successfully applied for real-time fluorescence monitoring of CDK9-catalyzed phosphorylation. This was enabled by the cooperative action of both binding sites of the hybrid biosensor, i.e., the native WW domain and the artificial Zn(II)−Dpa-based chemosensor unit. The incorporated chemosensor unit acts as not only a sensing probe but also a supportive

(25) Tamrakar, S.; Kapasi, A. J.; Spector, D. H. *J. Virol.* **2005**, *79*, 15477.

(26) Ashimori, A.; Ono, T.; Uchida, T.; Ohtaki, Y.; Fukaya, C.; Watanabe, M.; Yokoyama, K. *Chem. Pharm. Bull.* **1990**, *38*, 2446−2458.

sub-binding site. We believe that the hybrid approach is powerful in designing protein-based bioanalytical tools for structurally complicated targets of biological significance. For example, the sensing of various natural phosphoproteins may be carried out using a library of biosensors that are produced by combining suitable phosphoprotein binding domains with various suitable chemosensors so as to facilitate the understanding of specific protein phosphorylation−dephosphorylation events in detail. Toward this goal, we are now in progress along this line.

Experimental Section

Synthesis of 1−Zn(II). 4-Ethenyl-*tert*-butoxycarbonyl-aminobenzene (2). A solution of 4-aminostyrene (5.0 g, 42 mmol) and di-*tert*-butyl dicarbonate (18.3 g, 84 mmol) in dry CH_2Cl_2 (30 mL) was stirred for 14 h at room temperature. After dilution with CH_2Cl_2, the mixture was washed with 1 N HCl aq and brine followed by drying over anhydrous $MgSO_4$. The solvent was concentrated in vacuo to give compound **2** as a colorless solid in 98% yield (8.53 g): ^{1}H NMR ($CDCl_3$, 400 MHz) δ 7.33 (m, 4H, Ar-*H*), 6.62 (dd (10.8, 17.6), 1H, ethylene), 6.44 (br, 1H, amide), 5.65 (d(17.6), 1H, ethylene(trans)), 5.16 (d(10.8), 1H, ethylene(cis)), 1.52 (s, 9H, Boc).

4-[2-(6-Acetoxymethyl-4-pyridinyl)ethenyl]-*tert*-butoxycarbonyl-aminobenzene (4). A solution of **2** (1.24 g, 5.65 mmol), **3**[24] (1.0 g, 4.35 mmol), palladium acetate (195 mg, 0.87 mmol), and triphenylphosphine (456 mg, 1.74 mmol) in dry DMF (30 mL) was stirred for 22 h at 80 °C. After removal of the solvent in vacuo, the residue was dissolved in ethyl acetate (150 mL). The organic layer was washed with brine, dried over anhydrous $MgSO_4$, and concentrated by evaporation. The residue was purified by column chromatography on silica gel (hexane/AcOEt = 2/1) to give **4** as a light-brown oil in 56% yield (885 mg): ^{1}H NMR ($CDCl_3$, 400 MHz) δ 8.54 (d(4.8), 1H, Ar-*H*), 7.40−7.47 (m, 6H, Ar-*H*), 7.27 (d(16.4), 1H, ethylene(trans)), 6.67 (d(16.4), 1H, ethylene(trans)), 6.54 (br, 1H, amide), 5.23 (s, 2H, Ar-CH_2-O), 2.19 (s, 3H, COO-CH_3), 1.52 (s, 9H, Boc).

4-[2-(6-Hydroxymethyl-4-pyridinyl)ethenyl]-*tert*-butoxycarbonyl-aminobenzene (5). A solution of **4** (300 mg, 0.814 mmol) in 1 N NaOH aq (7 mL) and MeOH (10 mL) was stirred for 14 h at room temperature. The reaction mixture was diluted with H_2O and extracted with ethyl acetate. The organic layer was washed with brine, dried over anhydrous $MgSO_4$, and concentrated in vacuo to give compound **5** as a yellow oil in 76% yield (200 mg): ^{1}H NMR ($CDCl_3$, 400 MHz) δ 8.54 (d(4.8), 1H, Ar-*H*), 7.67 (m, 1H, Ar-*H*), 7.48 (m, 2H, Ar-*H*), 7.36 (m, 1H, Ar-*H*), 7.30 (m, 6H, Ar-*H*), 7.47 (m, 6H, Ar-*H*), 7.22 (d(16.4), 1H, ethylene(trans)), 6.91 (d(16.4), 1H, ethylene(trans)), 6.55 (br, 1H, amide), 4.77 (s, 2H, Ar-CH_2-O), 2.56 (s, 1H, OH), 1.52 (s, 9H, Boc).

4-[2-(6-Formyl-4-pyridinyl)ethenyl]-*tert*-butoxycarbonyl-aminobenzene (6). A suspension of **5** (200 mg, 0.61 mmol) and manganese dioxide (850 mg, 9.77 mmol) in dry THF (25 mL) was stirred for 2.5 h at room temperature and then for 1 h at 45 °C. The reaction mixture was filtered through celite, and the filtrate was concentrated in vacuo. The residue was purified by column chromatography on silica gel (hexane/AcOEt = 2/1) to give compound **6** as a yellow solid in 80% yield (158 mg): ^{1}H NMR ($CDCl_3$, 400 MHz) δ 10.10 (s, 1H, Ar-*H*), 8.71 (d(5.2), 1H, Ar-*H*), 8.04 (s, 1H, Ar-*H*), 7.53 (m, 3H, Ar-*H*), 7.41 (m, 2H, Ar-*H*), 7.35 (m, 1H, Ar-*H*), 6.98 (m, 1H, Ar-*H*), 6.58 (m, 1H, Ar-*H*), 1.54 (s, 9H, Boc).

4-(2-{6-[2-(Methylaminomethyl)pyridinyl]-4-pyridinyl}ethenyl)-*tert*-butoxycarbonyl-aminobenzene (7). A solution of **6** (94 mg, 0.29 mmol), 2-(methylaminomethyl)pyridine hydrochloride (40 mg, 0.33 mmol), acetic acid (20 mL, 0.30 mmol), and sodium triacetoxyborohydride (154 mg, 0.73 mmol) in dry CH_2Cl_2 (30 mL) was stirred for 6 h at room temperature. After dilution with CH_2Cl_2, the organic layer was washed with sat. $NaHCO_3$ aq and brine, followed by drying over anhydrous $MgSO_4$. The solvent was removed in vacuo, and the residue was purified by column chromatography on silica gel ($CHCl_3$/MeOH/NH_3 aq = 100/10/1) to give **7** as a yellow solid in 47% yield (58 mg): ^{1}H NMR ($CDCl_3$, 400 MHz) δ 8.57 (m, 1H, Ar-*H*), 8.48 (d(5.2), 1H, Ar-*H*), 7.67 (m, 1H, Ar-*H*), 7.59 (s, 1H, Ar-*H*), 7.49−7.51 (m, 3H, Ar-*H*), 7.39 (m, 2H, Ar-*H*), 7.29 (m, 1H, Ar-*H*), 7.21 (m, 1H, Ar-*H*), 7.16 (m, 1H, Ar-*H*), 6.93 (d(16.4, ethylene(trans)), 6.54 (m, 1H, Ar-*H*), 3.78 (s, 4H, Ar-*H*), 2.35 (s, 3H, Ar-*H*), 1.53 (s, 9H, Boc).

4-(2-{6-[2-(Methylaminomethyl)pyridinyl]-4-pyridinyl}ethenyl)-aminobenzene (8). A solution of **7** (112 mg, 0.26 mmol) in TFA (4 mL), and dry CH_2Cl_2 (12 mL) was stirred for 1 h at room temperature. After removal of the solvent in vacuo, the residue was dissolved in CH_2Cl_2 (50 mL). The organic layer was washed with sat. $NaHCO_3$ aq and brine followed by drying over anhydrous $MgSO_4$. The solution was concentrated in vacuo to give **8** as a brown oil in 80% yield (70 mg): ^{1}H NMR ($CDCl_3$, 400 MHz) δ 8.57 (m, 1H, Ar-*H*), 8.45 (d(5.2), 1H, Ar-*H*), 7.66 (m, 1H, Ar-*H*), 7.55 (s, 1H, Ar-*H*), 7.52 (m, 1H, Ar-*H*), 7.36 (d(8.4), 2H, Ar-*H*), 7.24 (d(16.4), 1H, ethylene(trans)), 7.20 (m, 2H, Ar-*H*), 6.83 (d(16.4), 1H, ethylene(trans)), 6.70 (d(8.4), 2H, Ar-*H*), 3.80 (m, 4H, Ar-CH_2-N), 2.36 (s, 3H, N-CH_3).

4-(2-{6-[2-(Methylaminomethyl)pyridinyl]-4-pyridinyl}ethenyl)-benzmaleimide (1). A solution of **8** (70 mg, 0.21 mmol) and maleic anhydride (31.2 mg, 0.318 mmol) in dry THF (15 mL) was stirred for 2 h at 40 °C. After removal of the solvent in vacuo, the residue was dissolved in acetic anhydride (8 mL). Sodium acetate (43.5 mg, 0.530 mmol) was added, and the mixture was stirred for 6 h at 60 °C. After dilution with AcOEt, the organic layer was washed with sat. $NaHCO_3$ aq and brine, followed by drying over anhydrous $MgSO_4$. The solvent was removed by evaporation, and the residue was purified by column chromatography on silica gel ($CHCl_3$/MeOH/NH_3 aq = 200/20/1) to give **1** as yellow solid in 53% yield (46 mg): ^{1}H NMR ($CDCl_3$, 400 MHz) δ 8.59 (m, 1H, Ar-*H*), 8.53 (d(5.2), 1H, Ar-*H*), 7.62−7.71(m, 4H, Ar-*H*), 7.52 (d(8.4), 1H, Ar-*H*), 7.41 (d(8.4), 2H, Ar-*H*), 7.34 (d(16.4), 1H, ethylene(trans)), 7.20 (m, 1H, Ar-*H*), 7.04 (d(16.4), 1H, ethylene(trans)), 6.88 (s, 2H, Ar-*H*), 3.80 (s, 4H, Ar-CH_2-N), 2.42 (s, 3H, N-CH_3). FAB-MS (NBA): calcd for $C_{25}H_{23}N_4O_2^+$ ($[M + H]^+$) 411.70, found 411.70.

4-(2-{6-[2-(Methylaminomethyl)pyridinyl]-4-pyridinyl} ethenyl)-benzmaleimide Zinc Complex (1−Zn(II)). An aqueous solution of zinc nitrate (306 mM; 370 μL, 0.113 mmol) was added to the solution of **1** (46.4 mg, 0.113 mmol) in distilled MeOH (4.7 mL), and the mixture was stirred for 30 min at room temperature. After removal of the solvent in vacuo, the residue was dissolved in distilled water and filtered through a cellulose acetate filter. The filtrate was lyophilized, and the obtained solid was filtered and washed with AcOEt to give **1**−Zn(II) as pale-yellow solid in 74% yield (50.3 mg): ^{1}H NMR (D_2O, 400 MHz) δ 8.55 (br, 1H, Ar-*H*), 8.44 (br, 1H, Ar-*H*), 7.58−7.69 (m, 4H, Ar-*H*), 7.54 (br, 1H, Ar-*H*), 7.43 (br, 2H, Ar-*H*), 7.35 (d(16.8), 1H, ethylene(trans)), 7.30 (m, 1H, Ar-*H*), 7.28 (br, 1H, Ar-*H*), 7.24 (m, 1H, Ar-*H*), 6.91 (s, 2H, Ar-CH_2-N), 3.96 (s, 4H, Ar-CH_2-N), 2.25 (s, 3H, N-CH_3). FAB-MS (NBA): calcd for $C_{25}H_{22}N_5O_5^+$ ($[M - NO_3]^+$) 537.86, found 537.43. Anal. Calcd for $C_{25}H_{22}N_4O_2 \cdot 2Zn(NO_3)_2 \cdot H_2O$; C 50.06, H 3.70, N 14.01. Found: C 50.19, H 3.53, N 14.09.

Synthesis of the Phosphopeptides. The peptide coupling reaction was performed with an automated peptide synthesizer (ABI 433A, Applied Biosystems). The peptides were synthesized using the standard Fmoc-based FastMoc coupling chemistry (0.1 mmol scale) on Fmoc-Amide Resin (Applied Biosystems). Fmoc-Ser[PO(Obzl)OH]-OH or Fmoc-Tyr[PO(Obzl)OH]-OH (Watanabe Chemical Industries, Ltd.) was used as a phosphorylated amino acid unit for the peptide coupling. The peptide cleavage from resin and side-chain deprotection were carried out by the treatment with TFA−*m*-cresol−thioanisole (86:2:12) over 1 h at rt. After removal of TFA in vacuo, the crude peptide was precipitated in *tert*-butylmethyl ether and purified by reversed-phase HPLC (column: YMC-pack ODS-A, 10 mm × 250 mm). Purification conditions were as follows: mobile phase, CH_3CN (0.1% TFA)/H_2O (0.1% TFA)) 5/95 to 24/76 (linear gradient over 25 min);

flow rate, 3.0 mL/min; detection, UV (220 nm). MALDI-TOF mass pS6,9-CTD: calcd for $C_{47}H_{70}N_{12}O_{25}P_2$ $[M - H]^-$ 1268.1, found 1266.6; pS6-CTD: calcd for $C_{47}H_{71}N_{12}O_{22}P$ $[M - H]^-$ 1188.1, found 1187.2; pS9-CTD: calcd for $C_{47}H_{71}N_{12}O_{22}P$ $[M - H]^-$ 1188.1, found 1189.1; S-CTD: calcd for $C_{47}H_{72}N_{12}O_{19}$ $[M + H]^+$ 1110.1, found 1109.1; IRK1P: calcd for $C_{74}H_{111}N_{20}O_{27}P$ $[M + H]^+$ 1743.8, found 1745.1; IRK2P: calcd for $C_{74}H_{112}N_{20}O_{30}P_2$ $[M + H]^+$ 1823.7, found 1823.8.

Synthesis of the Pin1 WW Domains. The peptide coupling reaction was performed with an automated peptide synthesizer (ABI 433A, Applied Biosystems). The Pin1 native WW domain (6−39; Native WW) and its cysteine mutants were synthesized using the standard Fmoc-based FastMoc coupling chemistry (0.25 mmol scale) on Alko-PEG Resin preloaded with Fmoc-Glycine (0.1 mmol, loading rate: 0.22 mmol/g, purchased from Watanabe Chemical Industries, Ltd.). After cleavage from resin and side-chain deprotection, the crude peptide was purified by reversed-phase HPLC. Purification conditions were as follows: reversed phase HPLC (column: YMC-pack ODS-A, 10 mm × 250 mm), mobile phase, CH_3CN (0.1% TFA)/ H_2O (0.1% TFA)) 20/80 to 40/60 (linear gradient over 30 min); flow rate, 3.0 mL/min; detection, UV (220 nm). MALDI-TOF mass (matrix; CHCA): calcd for native WW domain; $[M + H]^+$ 4025.1, found 4024.6, E12C-WW; calcd for $[M + H]^+$ 3997.5, found 3998.1, R14C-WW; calcd for $[M + H]^+$ 3970.5, found 3971.9, M15C-WW; calcd for $[M + H]^+$ 3995.5, found 3995.9.

Preparation of the Hybrid Biosensor 1(Zn)−M15C-WW. A solution of **1**−Zn(II) (185 μM in DMSO/H_2O (1:1), 83 μL) was slowly added to a solution of M15C-WW (123 μM, 1 mL) in 50 mM HEPES buffer (pH 7.2), and the mixture was incubated for 2 h at room temperature in a dark room. The reaction was monitored by MALDI-TOF-MS, in which the peak of M15C-WW disappeared and a new peak of **1**(Zn)−M15C-WW appeared (Figure S1). The reaction was also able to be monitored by UV−vis spectroscopy, in which the absorption maximum corresponding to the stilbazole unit of **1**−Zn(II) was red-shifted from 324 to 331 nm with an isosbestic point at 340 nm (Figure S1). The reaction solution was directly submitted to gel filtration chromatography (Sephadex G-25, 1.8 cm × 5 cm, 50 mM HEPES buffer (pH 7.2) as a eluant), and the fraction of **1**(Zn)−M15C-WW was collected. The concentration of **1**(Zn)−M15C-WW was determined by absorbance at 340 nm ($\epsilon_{340} = 6245$ M^{-1} cm^{-1}) or 280 nm ($\epsilon_{280} = 14{,}640$ M^{-1} cm^{-1}), where the absorption coefficient (ϵ) at each wavelength was determined based on the ϵ of **1**−Zn(II) or the sum of the ϵ of **1**−Zn(II) and the native WW domain, respectively. MALDI-TOF mass; *m*/*z* calcd for 4595.4, found 4534.1.

Circular Dichroism Measurement. CD spectra were recorded using a JASCO J-720W spectropolarimeter. The aqueous solution of the WW domain (4.6 μM) in 20 mM phosphate buffer (pH 7.2) was prepared, and CD spectra were measured from 300 to 200 nm (scan speed; 50 nm/min) at 4 °C using a water-jacketed quartz cell (0.1 cm path length). Each spectrum represents the average of 16 time scans with smoothing to reduce noise.

Fluorescence Titration with Phosphate Derivatives. Fluorescence spectra were recorded on a Perkin-Elmer LS55 spectrometer. The titration experiments were conducted with a solution of **1**(Zn)−M15C-WW (3.2 μM) in 50 mM HEPES buffer (pH 7.2). All titration were carried out with **1**(Zn)−M15C-WW solution (0.5 mL) in a quartz cell (excitation wavelength: $\lambda_{ex} = 340$ nm,) at 15 ± 1 °C, and the fluorescence emission was recorded upon addition of a freshly prepared aqueous stock solution of the peptide or phosphate species with a microsyringe. Fluorescence titration curves ($\lambda_{em} = 440$ nm) were analyzed with the nonlinear least-squares curve-fitting method asumming 1:1 binding to give the apparent binding constant (K_{app}, M^{-1}).

Fluorescence Anisotropy Experiment. Fluorescence anisotropy experiments were performed with a Perkin-Elmer LS55 spectrometer. The fluorescence anisotropy value (*r*) of **1**(Zn)−M15C-WW was calculated by eq 1 using the emission intensity at 441 nm, where I_{VV}, I_{VH}, I_{HV}, and I_{HH} are the fluorescence intensities observed through polarizers parallel and perpendicular to the polarization of the exciting light, respectively, and *G* is a correction factor accounting for instrumental differences in the fluorescence detection.

$$r = (I_{VV} - GI_{VH})/(I_{VV} + 2GI_{VH}) \quad G = I_{HV}/I_{HH} \tag{1}$$

Fluorescence Monitoring of CDK9/T1-Catalyzed Phosphorylation. CDK9/T1 (human, recombinant) was purchased from Upstate. The preincubated solution of **1**(Zn)−M15C-WW (3.2 μM), ATP (50 mM) and CDK9/T1 (50 mU) in the assay buffer (8 mM MOPS, pH 7.0, 1 mM $MgCl_2$, 100 mM $ZnCl_2$ containing 20% glycerol) at 20 ± 1 °C was mixed with pS-9 CTD peptide (final concentration: 50−400 μM), and the fluorescence spectrum (excitation wavelength: $\lambda_{ex} = 340$ nm) was monitored at 20 ± 1 °C with the kinetic mode from 0 to 60 min. Changes in the fluorescence intensity at 440 nm were converted to the initial rate (v_i, $M \cdot min^{-1}$) by using the calibration curves obtained from the fluorescence titration under the assay conditions. The data were analyzed by Lineweaver−Burk equation to obtain Michaelis constant [V_{max} ($M \cdot min^{-1}$), K_m (M)]. At the same time, the phosphorylation reaction was also traced by MALDI-TOF-MS. All of the control experiments in the absence of ATP, pS-9 CTD peptide or CDK9/T1 kinase, and the kinase reaction with non-phosphorylated CTD peptide were also conducted under the same reaction conditions.

Supporting Information Available: Figures S1−S5 showing additional experimental details. This material is available free of charge via the Internet at http://pubs.acs.org.

JA0693284